Durham University

Durham Research Online

Deposited in DRO:

01 July 2015

Version of attached file:

Published Version

Peer-review status of attached file:

Peer-reviewed

Citation for published item:

Slater, C. T. and Bell, E. F. and Schlafly, E. F. and Morganson, E. and Martin, N. F. and Rix, H.-W. and Peñarrubia, J. and Bernard, E. J. and Ferguson, A. M. N. and Martinez-Delgado, D. and Wyse, R. F. G. and Burgett, W. S. and Chambers, K. C. and Draper, P. W. and Hodapp, K. W. and Kaiser, N. and Magnier, E. A. and Metcalfe, N. and Price, P. A. and Tonry, J. L. and Wainscoat, R. J. and Waters, C. (2014) 'The complex structure of stars in the outer Galactic disk as revealed by Pan-STARRS1.', Astrophysical journal., 791 (1). p. 9.

Further information on publisher's website:

http://dx.doi.org/10.1088/0004-637X/791/1/9

Publisher's copyright statement:

© 2014. The American Astronomical Society. All rights reserved.

Additional information:

Use policy

The full-text may be used and/or reproduced, and given to third parties in any format or medium, without prior permission or charge, for personal research or study, educational, or not-for-profit purposes provided that:

- a full bibliographic reference is made to the original source
- a link is made to the metadata record in DRO
- the full-text is not changed in any way

The full-text must not be sold in any format or medium without the formal permission of the copyright holders.

Please consult the full DRO policy for further details.

Durham University Library, Stockton Road, Durham DH1 3LY, United Kingdom
Tel : +44 (0)191 334 3042 | Fax : +44 (0)191 334 2971
https://dro.dur.ac.uk

The Astrophysical Journal, 791:9 (8pp), 2014 August 10 doi:10.1088/0004-637X/791/1/9
© 2014. The American Astronomical Society. All rights reserved. Printed in the U.S.A.

THE COMPLEX STRUCTURE OF STARS IN THE OUTER GALACTIC DISK AS REVEALED BY PAN-STARRS1

Colin T. Slater[1], Eric F. Bell[1], Edward F. Schlafly[2], Eric Morganson[3], Nicolas F. Martin[2,4], Hans-Walter Rix[2], Jorge Peñarrubia[5], Edouard J. Bernard[5], Annette M. N. Ferguson[5], David Martinez-Delgado[6], Rosemary F. G. Wyse[7], William S. Burgett[8], Kenneth C. Chambers[8], Peter W. Draper[9], Klaus W. Hodapp[8], Nicholas Kaiser[8], Eugene A. Magnier[8], Nigel Metcalfe[9], Paul A. Price[10], John L. Tonry[8], Richard J. Wainscoat[8], and Christopher Waters[8]
[1] Department of Astronomy, University of Michigan, 500 Church Street, Ann Arbor, MI 48109, USA; mailto:ctslater@umich.edu, ctslater@umich.edu, mailto:ericbell@umich.edu
[2] Max-Planck-Institut für Astronomie, Königstuhl 17, D-69117 Heidelberg, Germany
[3] Harvard-Smithsonian Center for Astrophysics, 60 Garden Street, Cambridge, MA 02138, USA
[4] Observatoire astronomique de Strasbourg, Université de Strasbourg, CNRS, UMR 7550, 11 rue de l'Université, F-67000 Strasbourg, France
[5] Institute for Astronomy, University of Edinburgh, Royal Observatory, Blackford Hill, Edinburgh EH9 3HJ, UK
[6] Astronomisches Rechen-Institut, Zentrum für Astronomie der Universität Heidelberg, Mönchhofstr. 12-14, D-69120, Heidelberg, Germany
[7] Department of Physics and Astronomy, Johns Hopkins University, 3400 North Charles Street, Baltimore, MD 21218, USA
[8] Institute for Astronomy, University of Hawaii at Manoa, Honolulu, HI 96822, USA
[9] Department of Physics, Durham University, South Road, Durham DH1 3LE, UK
[10] Department of Astrophysical Sciences, Princeton University, Princeton, NJ 08544, USA
Received 2014 April 16; accepted 2014 June 24; published 2014 July 21

ABSTRACT

We present a panoptic view of the stellar structure in the Galactic disk's outer reaches commonly known as the Monoceros Ring, based on data from Pan-STARRS1. These observations clearly show the large extent of the stellar overdensities on both sides of the Galactic disk, extending between $b = -25^\circ$ and $b = +35^\circ$ and covering over 130° in Galactic longitude. The structure exhibits a complex morphology with both stream-like features and a sharp edge to the structure in both the north and the south. We compare this map to mock observations of two published simulations aimed at explaining such structures in the outer stellar disk, one postulating an origin as a tidal stream and the other demonstrating a scenario where the disk is strongly distorted by the accretion of a satellite. These morphological comparisons of simulations can link formation scenarios to observed structures, such as demonstrating that the distorted-disk model can produce thin density features resembling tidal streams. Although neither model produces perfect agreement with the observations—the tidal stream predicts material at larger distances that is not detected while in the distorted disk model, the midplane is warped to an excessive degree—future tuning of the models to accommodate these latest data may yield better agreement.

Key words: galaxies: evolution – galaxies: interactions – Galaxy: disk – Galaxy: structure

Online-only material: color figures, supplemental data

1. INTRODUCTION

The stellar overdensity usually termed the Monoceros Ring (MRi) has been studied for over a decade, but remains a poorly understood phenomenon in the outer Galactic disk. First identified by Newberg et al. (2002) and later shown prominently by Yanny et al. (2003) and Belokurov et al. (2006), in the Sloan Digital Sky Survey (SDSS) the structure appears as an overdensity of stars at ∼10 kpc from the Sun, spanning Galactic latitudes from $b \sim +35^\circ$ to the edge of the SDSS footprint of $b \sim +20^\circ$ and in Galactic longitude extending between $l = 230^\circ$ and $l = 160^\circ$.

As the initial detections were widely separated but approximately centered on the constellation Monoceros, and it appeared to lie at a constant Galactocentric distance, it was termed the MRi.[11] Subsequent studies based on modest numbers of photometric pointings have elucidated the distance dependence of the structure and provided pencil beam mappings of the structure (e.g., Ibata et al. 2003; Conn et al. 2005a; Vivas & Zinn 2006; Conn et al. 2007, 2008, 2012; Li et al. 2012). These pointings have also shown that the feature appears both north and south of the Galactic plane at similar Galactic longitudes (Conn et al. 2005a; de Jong et al. 2010), further expanding the known size of the structure. A summary of many of the detections of the MRi is shown in Figure 1, along with the main-sequence turn-off (MSTO) stellar density map from the SDSS showing the MRi detections within its footprint. Spectroscopic observations have shown that much of the MRi is consistent with a nearly circular orbit at a velocity of ∼220 km s^{-1} (Crane et al. 2003; Conn et al. 2005b; Martin et al. 2006) and have potentially identified related star clusters at similar velocities (Frinchaboy et al. 2004). The association between the MRi and other density structures in the Galactic disk and halo has been the source of considerable controversy, with the Canis Major overdensity (Martin et al. 2004) and the Triangulum–Andromeda overdensity (Rocha-Pinto et al. 2004) both lying near detections of the MRi, and with debate as to whether the density structure seen in SDSS is of a common origin or multiple distinct structures (Grillmair 2006; Grillmair et al. 2008).

While the basic observations of the MRi are generally agreed on, there is very little consensus on details beyond these, and particularly in the origin of the structure, there is wide disagreement. One possibility is that the MRi is the tidal debris from a disrupting dwarf satellite galaxy (Martin et al. 2004; Peñarrubia et al. 2005; Sollima et al. 2011). In this scenario, the stream's orbital plane is similar to that of the Galactic disk by virtue of a low-inclination progenitor orbit. An alternative

[11] Though, the structure clearly extends beyond the borders of the constellation Monoceros, we retain this terminology for convenience herein.

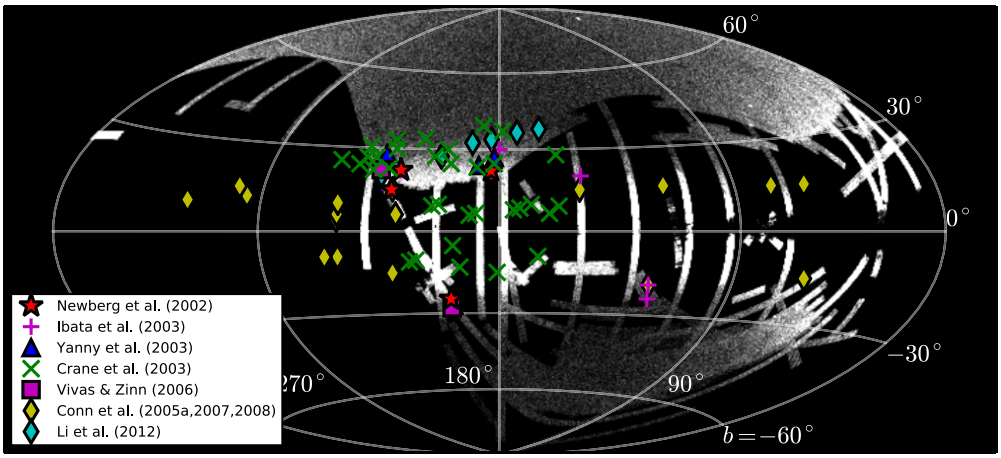

Figure 1. Comparison of previous detections of the MRi from various authors (each listed in the figure legend), overlaid on the map of the MRi as seen by the SDSS (showing the density of stars with $0.2 < (g-r)_0 < 0.4$ and $18.6 < g_0 < 19.8$). While the individual pointings clearly show that the MRi occupies a significant amount of area in the Galactic anticenter, both north and south of the Galactic plane, it is difficult to understand the morphology of the structure without contiguous imaging coverage.

(A color version of this figure is available in the online journal.)

scenario is that the stars in the MRi originally formed in the Galactic disk, but were stirred up by some dynamical perturbation to heights of 1–5 kpc above and below the disk. Qualitatively, such scenarios can be simply stated, but their parameterization and characterization can be complex.

Some models have sought to characterize the observations of overdensity by modeling a flare and a warp in the Galactic stellar disk (Momany et al. 2006; Hammersley & López-Corredoira 2011), while numerical models have sought to recreate an MRi-like feature in *N*-body simulations by perturbing a disk with satellite galaxies (Younger et al. 2008; Kazantzidis et al. 2008). Perturbations to the disk by satellites have been studied both in observations (Widrow et al. 2012) and in *N*-body simulations of spiral arms (Purcell et al. 2011) and vertical density waves (Gómez et al. 2013), all reinforcing the picture that the disk can exhibit complex structure in response to close satellite passages. Observationally, in M31 disk-like stellar populations have been found at large distances from the bright stellar disk (Richardson et al. 2008), and appear to also have disk-like kinematics (Ibata et al. 2005). Distortions and warps in the outer stellar disks and H I gas of galaxies appear common (Sanchez-Saavedra et al. 1990; García-Ruiz et al. 2002), and some have been shown to cause the formation of young stars at large heights from the plane as defined by the central region of the galaxy (Radburn-Smith et al. 2014).

Most of the models of the MRi can produce qualitative matches to the available data, which has left little leverage to distinguish between these scenarios. In particular, the lack of a contiguous map of the MRi has forced models to rely on matching the distances and depth of the structure as seen by the available sparse pointings. This limited data set has made it difficult to see a correspondence (or disagreement) between the *N*-body simulations and the actual MRi structure, since the complex density structure predicted by these simulations can be masked when only a limited number of discontiguous pointings are available for comparison.

In this work, we present a panoramic view of the MRi using Pan-STARRS1 (PS1; Kaiser et al. 2010) extending both north and south of the Galactic disk and covering 160° in Galactic longitude. This is the most comprehensive map of the MRi to date, enabled by extensive sky coverage of PS1 and its survey strategy that—unlike SDSS—fully includes the Galactic plane. As we will show, this panoptic view provides a dimension of spatial information that had previously only been hinted at and incomplete, particularly in the southern Galactic hemisphere.

To illustrate the utility of these new maps, we also present a first comparison to physically motivated *N*-body simulations. Though qualitative in nature, we will show that such comparisons can immediately be used to refine our understanding of the physical ingredients necessary for reproducing the structure. In the following work we describe the PS1 survey and the data processing in Section 2, followed by a discussion of the resulting MRi maps in Section 3. We show the comparisons to the two *N*-body models in Section 4, and we discuss the results and conclusions in Section 5.

2. THE PAN-STARRS1 DATA

PS1 is a 1.8 m telescope on the summit of Haleakela, Hawaii, which operates as a dedicated survey instrument (K. C. Chambers et al., in preparation). The telescope images in five bands ($g_{\rm P1}r_{\rm P1}i_{\rm P1}z_{\rm P1}y_{\rm P1}$) with average exposure times on the order of 30–45 s (Metcalfe et al. 2013). The individual exposures are photometered by an automated pipeline (Magnier 2006) and calibrated to each other self-consistently using partially overlapping exposures (Schlafly et al. 2012), yielding a calibration precision better than 10 mmag as measured against SDSS. In this work we use data from the 3π survey, which covers the entire sky north of declination $-30°$ and is designed to obtain approximately four exposures per pointing, per filter, per year. Although the survey does produce stacked images and the resulting photometry, in this work we use data that is the merger of the photometric catalogs of all individual exposures. Stacked data from PS1 will reach more than a magnitude deeper, but the processing pipeline for the single epoch data is currently more mature and reliable. MSTO stars in Monoceros are easily detected in the PS1 single epoch images, and so we accordingly use that data in this work. We use the most recent consistent reprocessing of the 3π observations, termed Processing Version 1, which contains observations obtained primarily between 2010 May and 2013 March. As measured against the SDSS stripe 82 coadd catalog, our 50% completeness levels range from roughly $g_{\rm P1} = 21.4$ to 22.0, and $r_{\rm P1} = 21.2$ to 21.8 (Slater et al. 2013). Since these are limits are substantially fainter than our target

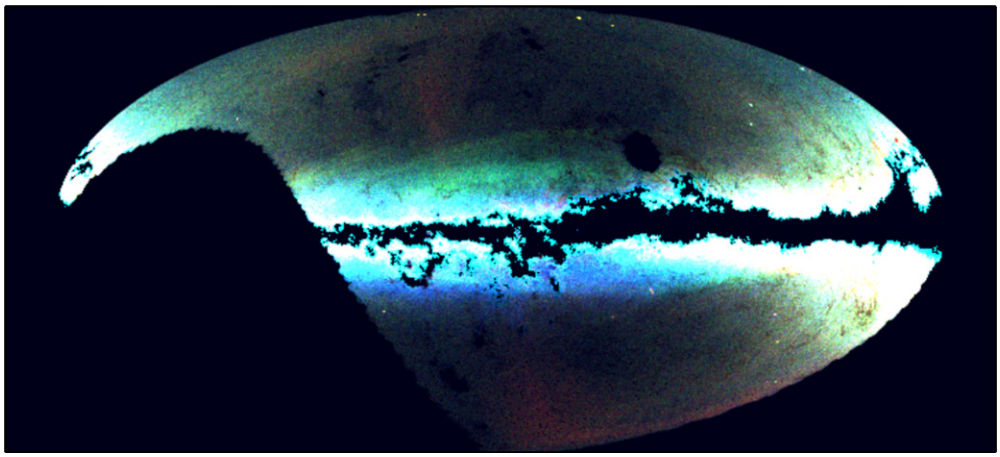

Figure 2. Pan-STARRS1 map of star counts in Galactic coordinates for stars with $0.2 < (g-r)_0 < 0.3$. Nearby stars with $17.8 < g_0 < 18.4$ (4.8–6.3 kpc) are shown in blue, stars with $18.8 < g_0 < 19.6$ (7.6–11.0 kpc) are shown in green, and more distant stars with $20.2 < g_0 < 20.6$ (14.4–17.4 kpc) are shown in red. The Galactic anticenter is in the middle, and the Galactic center is on the right edge. The MRi can clearly be seen in broadly horizontal green structure on the northern side of the plane and in the similar structure on the southern side of the plane in blue, both of which extend over 130° in Galactic longitude. The difference in color as presented suggests that the southern component is slightly closer to the Sun than the northern component. The Galactic plane and some localized regions near the plane are missing due to high extinction, while the apparent hole near the north celestial pole was imaged but not included in this processing of the data. There are some regions of the north Galactic cap and near the celestial pole that suffer from poor PS1 coverage. The Sagittarius stream appears nearly vertical in red on both sides of the disk.
(A color version and supplemental data of this figure are available in the online journal.)

MSTO stars in the MRi, this limited photometric depth will not impair our results.

Because the stars used we focus on in this work are much brighter than the completeness limit, our photometric uncertainties are largely the result of large-scale systematic effects and calibration uncertainties rather than photon noise on the photometry itself. In general this results in a typical uncertainty of 0.01–0.02 mag (see Schlafly et al. 2012 for further details). The most significant remaining uncertainty is the correction for Galactic extinction. The relatively narrow color selection we use makes the number counts of MSTO stars sensitive to small color shifts, which can be caused by errors in the extinction maps used for dereddening. For extinction correction we use the maps of Schlegel et al. (1998), corrected with the factors prescribed by Schlafly & Finkbeiner (2011). While the Schlegel et al. (1998) maps are generally excellent, there are regions of our maps where changes in the measured stellar density correlate strongly with dust extinction features. This is primarily an issue within 20°–30° of the north celestial pole, and we therefore do not want to overinterpret the results there. Beyond this particular region the extinction correction appears to be well-behaved and there are fewer correlations between MSTO map features and extinction features. The regions where we have marked Monoceros-like features do not show significant dust features.

Here our principal objective with the PS1 observations is to create a series of stellar density maps showing the spatial extent and morphology of the MRi in a low-latitude version of the "Field of Streams" (Belokurov et al. 2006). To do this, we impose cuts on color and magnitude of stars in a way designed to select MSTO stars of an old (∼9 Gyr) population with $-1 \lesssim$ [Fe/H] $\lesssim 0$ and at the range of heliocentric distances of interest. A color range of $0.2 < (g-r)_0 < 0.3$ optimizes the contrast between the MRi and any foreground (nearby Galactic disk) or background (stellar halo) contamination. We have estimated the distance to the stars selected by this color cut with the BaSTI set of isochrones (Pietrinferni et al. 2004). We use a 9 Gyr old, [Fe/H] $= -1.0$ isochrone populated with a Kroupa (2001) initial mass function and with realistic observational uncertainties added. The choice of stellar population parameters are in line with the metallicity measured for the MRi by both Conn et al. (2012) and Meisner et al. (2012), though substantial scatter in the metallicity of the MRi has been reported (e.g., Yanny et al. 2003; Crane et al. 2003). The median magnitude of the synthesized stars selected by this color cut is $M_{g,\mathrm{P1}} = 4.4$, which we shall adopt for our quoted distances, though the spread is considerable and 70% of synthesized stars are found within ±0.5 mag of the median value. The uncertainty in the stellar populations of the MRi, particularly the age, adds an additional ∼0.2 mag systematic uncertainty, but this is substantially less than the intrinsic magnitude spread of the MSTO in a single stellar population. The uncertainty between different sources of isochrones is at a similar level, and studies of globular clusters also produce similar results (Newby et al. 2011).

3. OBSERVED MRi MORPHOLOGY

Figure 2 shows the MSTO stellar density map, projected in Galactic coordinates, centered on the Galactic anticenter. The components of the three-color image were chosen to show stars with $17.8 < g_0 < 18.4$ (centered on roughly 4.8–6.3 kpc, but also broadened by the intrinsic MSTO magnitude spread) in blue, stars with $18.8 < g_0 < 19.6$ in green (7.6–11.0 kpc), and more distant stars with $20.2 < g_0 < 20.6$ in red (14.4–17.4 kpc). These maps are available as FITS files in the online edition of the journal, along with the intermediate distance slices. The most prominent features of the MRi are the broad horizontal arcs on both the northern and southern sides of the disk, primarily in blue and green, showing several sharp density features at large heights above the disk. On the northern side multiple arcs are visible, which we have labeled in Figure 3 for convenience in describing them. The MRi features seen in SDSS are what we have labeled Features B and C, with some small part of Feature A also visible toward the edge of the SDSS coverage. Where the Pan-STARRS and the SDSS coverage overlap there is good agreement on the morphology of the features, while the additional new area available in the PS1 coverage shows all of

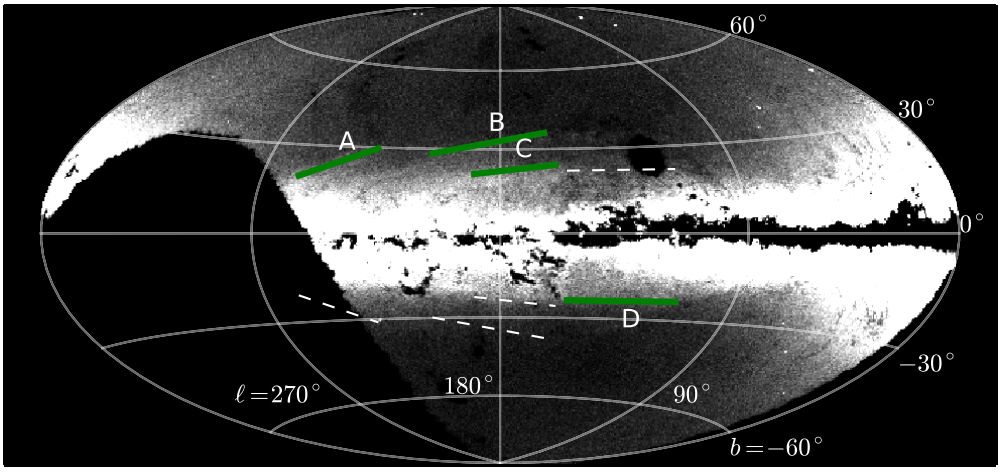

Figure 3. Same as Figure 2, showing the middle (green in Figure 2) distance slice and with several density features labeled. These markings are not intended to be comprehensive, and many of the features extend beyond the extent of the labels. The white dashed lines show the location of the labeled features reflected across the Galactic plane. The grid shows $l = 90°$ (right side), $l = 180°$, and $l = 270°$ (left side), along with lines at $b = \pm 30°$ and $\pm 60°$.

(A color version of this figure is available in the online journal.)

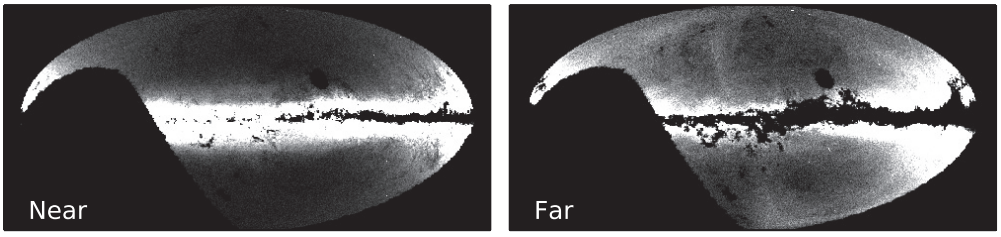

Figure 4. Two distance slices, one nearer than the main body of the MRi (left, shown in blue in Figure 2, $17.8 < g_0 < 18.4$) and one further (right, shown in red in Figure 2, $20.2 < g_0 < 20.6$). In the nearer slice there is very little evidence of the MRi in the north, though southern structure remains visible. In the far slice the MRi has become much less prominent and there is little new MRi-related structure that becomes apparent.

these features in a contiguous map, revealing that they extend substantially beyond the SDSS footprint.

The southern extent of the MRi has not been seen before in a wide-area map. The broad southern sharp-edged arc is strikingly similar to the observed arc on the northern side of the disk, particularly Feature C, and leaves little doubt that these features are related. In our maps the MRi clearly encompasses a vast area of the Galactic anticenter region, spanning from $b = -25°$ to $b = +35°$ and covering nearly 130° in longitude on both sides. It is interesting to note that the material that makes up Features C and D appears to blend smoothly in with the disk closer to the Galactic plane, with no second sharp edge at lower latitudes to denote an "end" of the MRi material. This is particularly apparent in the south, as some extinction features may be affecting the north slightly more.

Though the bulk of the MRi appears similar on both sides of the Galactic plane, there are small but noticeable asymmetries between the northern and southern features. To aid in seeing this, the marked features have also been reflected across the Galactic equator and denoted with dashed white lines. The A and B features clearly extend further off the Galactic plane than any feature in the south, though C and D seem to be very similar in extent both in latitude and longitude. There does not appear to be the same multiplicity of arcs on the southern side as compared to the north.

These arcs, which we refer to as Features A and B, have been previously pointed out by Grillmair (2006) and revisited in Grillmair (2011), which referred to these features as the anticenter stream and the eastern banded structure, respectively. Though these stellar density features certainly exist, their decomposition into "distinct" features does not appear obvious or unique.

In Figure 4 we show the nearer (blue in Figure 2) and farther (red in Figure 2) distance slices separately from Figure 2, so that they can be examined independently. These maps show that the structure is relatively well-confined in heliocentric distance, with the southern part becoming visible in the near slice and only hints of the structure remaining in the far slice. We will illustrate the utility of these distance slices for constraining models in Section 4, but from the data alone we can show that the structure is not very extended in heliocentric radius. There is, however, an offset in distance between the northern and southern components of the MRi, with the southern component somewhat closer to the Sun than the northern side.

4. MODEL COMPARISONS

In order to guide the understanding of the observed MRi, we have created "mock observations" of two *N*-body simulations. One of these models the MRi as perturbed disk stars that have been stirred up by satellite galaxies (Kazantzidis et al. 2009), while the other models the MRi as simply the debris from a disrupted satellite (Peñarrubia et al. 2005). These two simulations serve to illustrate the range of morphologies that these categories of models generate, along with demonstrating the utility of the PS1 maps for differentiating between these models. We note that at this stage neither simulation has been tuned to reproduce the PS1 observations, so discrepancies must

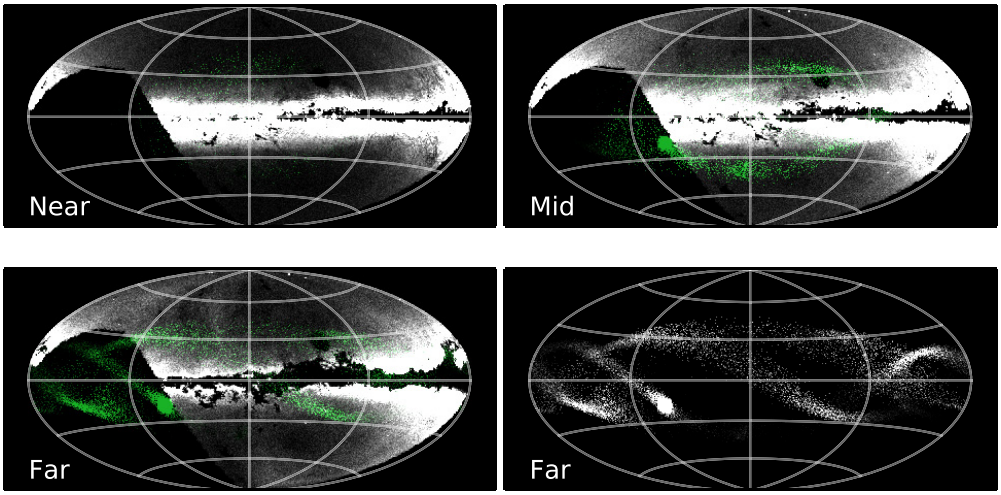

Figure 5. Visualization of the Peñarrubia et al. (2005) model for the formation of the MRi by accreted satellite material (green points), plotted on top of the PS1 observations. We show three magnitude slices (approximately corresponding to distance slices used in the observations), with the top right "mid" slice matching Figure 2 and the "near" (top left) and "far" (bottom left) slices matching Figure 4. The "far" simulation slice is repeated by itself on the bottom right for clarity. The PS1 images are the same as Figures 2 and 4. The "mid" slice shows broad agreement with the observed structure, though somewhat offset, while the "far" slice shows a considerably different set of overdensities that do not appear to match the observations.

(A color version of this figure is available in the online journal.)

be expected, but our goal is to highlight these discrepancies so that future models may be better tuned to match the observations.

To produce maps of the simulations with similar observational characteristics to the PS1 data, we use the same isochrones as in Section 2 to determine the extent to which each simulation particle contributes to the various magnitude slices, with the considerable magnitude spread of the MSTO causing simulation particles to potentially contribute to multiple slices. As per our population modeling in Section 2, we account for this spread by approximating the MSTO absolute magnitude distribution as a Gaussian centered on $M_{g,\mathrm{P1}} = 4.4$ and a width of 0.5 mag. This center and width approximate the synthesized distribution of MSTO stars, though in detail the shape likely deviates somewhat from a Gaussian. After determining each particle's contribution to a given magnitude slice, the particles are projected onto the "sky" as would be seen by an observer and summed to produce the star counts map. It is important to note that the simulations are run at resolutions much coarser than single stars, and hence individual simulation particles are visible in some regions of the maps, which contributes to a "grainy" appearance. We do not correct for this.

4.1. Satellite Accretion Model

As an example of models that recreate the MRi as the tidal debris of a dwarf galaxy, we show the simulations of Peñarrubia et al. (2005). This simulation attempted to reproduce all of the positions, distances and velocities of the MRi that were known at the time of publication. To do so, the authors varied the properties of the accreted dwarf along with its orbit and the shape of the Galactic potential to find a solution that best reproduced the known observations. The resulting best fit has the hypothesized dwarf on a very low-eccentricity orbit ($e \sim 0.1$) and at a low inclination relative to the Galactic plane, which allows it to make multiple wraps over a relatively narrow range of Galactocentric radii and relatively close to the disk in height. The simulation is also designed so that the main body of the disrupting satellite appears in the region of the Canis Major overdensity (Martin et al. 2004), as an attempt to link the two structures. As more recent evidence suggests that the Canis Major overdensity may not be related to a disrupted dwarf (Mateu et al. 2009), in our comparison we will focus on the general behavior of the tidal stream component rather than the specific location of the progenitor. Also note that this simulation focused on the properties of tidal debris, there are no *N*-body particles from the Galactic disk, which is instead modeled with a static potential. The particles used to reproduce the stream are the dark matter particles from the satellite, as there was no distinction made between a central concentration of luminous particles and a larger dark matter halo. As a result, the model predictions of the surface brightness of the stream along its orbit may be inaccurate, and further work would be needed to make more precise predictions. Our focus is thus on the general morphological comparison between the model and observations.

A visualization of the simulation can be seen in Figure 5 as green points (satellite debris particles) plotted on top of the observed PS1 data. Three magnitude slices are plotted, corresponding to the cut targeting the main body of the MRi in Figure 2 (labeled "mid") and the two cuts on the near side and far side of the MRi from Figure 4. From this we can see that the overall shape of the MRi is reproduced quite well in the "mid" distance slice of the simulation. The north and south both exhibit very broad structures with a sharp edge on the side away from the Galactic plane, along with a convincing degree of symmetry across the two hemispheres that is reminiscent of the symmetry of Features C and D.

Though the "mid" distance slice exhibits considerable resemblance (though with some spatial offset), there is substantial discrepancy between the simulation and the observed structure in the "far" slice. Some of the material in the far slice does trace northern and southern edges of the MRi as observed, but generally the material appears in new regions of the sky that were not as well-populated in the "mid" slice. This is noticeable in the south, where a broad stream paralleling the observed MRi in the "mid" slice is replaced by a different wrap of the stream at a different angle in the far slice, cutting across the plane rather than paralleling it. In the north the simulated MRi material is prominent in differing regions; while both match some portion of the MRi, the mid and far slices do not match each other. These

features are in contrast to the strong similarity between the observed mid and far slices, in which the far slice does not show any new features of MRi appearing that were not prominent in the mid slice. Some of the structures that appear most prominently at closer distances still appear in the far slice, due to the intrinsic spread in magnitude of the MSTO, but no new components of the MRi appear in the far slice. A portion of the features in the simulation do fall outside the PS1 footprint on the sky, particularly structures on the far left side of the figure, which corresponds to the southern celestial hemisphere, but there appears to be substantial structure even within the area covered by PS1. The recent deep mapping near Andromeda (Martin et al. 2014) may show some material resembling the stream model shown here (which they refer to as the "PAndAS MW stream," near $l = 120°$, $b = -20°$), but the detected material is further than both our "far" slice and the predicted stream, so the correspondence is tentative. The overdensity in the simulation between $l = 180°$ and $l = 270°$ and just south of the Galactic plane is the main body of the disrupting dwarf. We do not find an overdensity of this significance in the PS1 data, but this is mostly off the edge of the PS1 coverage and is also likely to be a specific prediction of this particular simulation rather than a general prediction of tidal stream models.

The general discrepancy between the simulation and the observed MSTO maps in the amount of structure at large distances may be intrinsic to satellite accretion models, which in general require dwarfs to be on at least mildly eccentric orbits and thus causing the widely spread debris. The challenge for future accretion models that attempt to reproduce the MRi is thus to plausibly explain the circular orbit, or to present some other way in which the debris at larger distances is hidden from view.

4.2. Disrupted Disk Model

The simulation of Kazantzidis et al. (2009) present a case where the disk of the galaxy has been strongly disrupted by the impact of satellite galaxies. The simulation we show is one of a suite of controlled experiments where a Milky Way-sized disk was subjected to bombardment by a cosmologically motivated set of six dark halos. These halos range from 20%–60% of the mass of the disk itself, with the majority of the effect on the disk being driven by the most massive accretion event. The disk in the simulation has a mass of $3.53 \times 10^{10} M_{\odot}$, and the satellite halos hence had masses ranging from $7.4 \times 10^{9}\ M_{\odot}$ to $2 \times 10^{10}\ M_{\odot}$. The pericenters of the satellite orbits ranged from 1.5 kpc to 18 kpc. In contrast to the Peñarrubia et al. (2005) model, in this visualization there are no particles from the dwarfs shown; the particles we show were all originally in the simulated disk.

While the transformation from simulation particles into "mock" MSTO slices is the same for this simulation as for our presentation of the Peñarrubia et al. (2005) simulation, there are a few additional complications. Because the Kazantzidis et al. (2009) simulation was not tuned to reproduce any observations of the MRi, there is no preferred position for the observer. That is, we can visualize the simulation as if we were at any point on the solar circle, each time obtaining a unique view of the disrupted disk. We chose an observer position that gives the best qualitative resemblance between the simulations and the observations in order to show as many positive features of this type of model as possible. There is also some question as to how best to define the Galactic plane in such a simulation. A gas disk would be the natural choice, but since this is an *N*-body only simulation, that option is not available. Following the initial analysis of the simulation in Kazantzidis et al. (2009), we have chosen to align the galactic plane of our visualization perpendicular to the total angular momentum axis summed over all of the particles in the simulation.

The resulting mock observations are shown in Figure 6, where a substantial warping of the disk is clearly evident. To the right of the anticenter there is very little material remaining along the Galactic equator, as nearly all of it has been displaced. This level of disk distortion is evident regardless of where the observer is placed along the solar circle. This level of disk warping is substantially beyond what is observed in the Galaxy, where the offset between the Galactic plane and peak density of the stellar disk is at most 1°–2° (Momany et al. 2006) rather than the ∼10° in the simulation.

Despite this drawback, we find the simulation to be very useful in showing the possible disk response morphologies generated by a substantial perturbation. There are very clear "streamers" visible that appear to fly off from the disk (in Figure 6 coincidentally overlapping where Feature A is), along with features of higher density and sharp edges up off the disk (near Features B and C). As discussed above, we have intentionally selected the position of the observer in this simulation to best highlight the agreement between the simulation and the observations, so we should not over-interpret this agreement as a conclusive statement about the origin of the MRi. The presence of such strikingly similar features should lend credibility to the hypothesis that the complex and highly structured MRi features in the Galaxy have a common origin, but only if the degree of disk disruption can be brought into line with observations.

Figure 7 shows the nearer and further distance slices of the Kazantzidis et al. (2009) model. The warp clearly extends across all of these distance slices, with somewhat lower projected heights in the more distant slice. However, these alternate slices show similar substructure as in the "mid" slice, with no morphologically distinct components becoming visible as is predicted by the Peñarrubia et al. (2005) model. On this basis the tidal stream model is more easily seen to be in conflict with the observations, but the disrupted disk may similarly be too extended in radius. A quantitative comparison of the radial extent of the simulated disruption with the observed MRi would be necessary to confirm this. The radial profile of the disrupted disk material may also depend strongly on the disk's initial profile, adding another degree of freedom to such models.

Based on these comparisons, the crucial question for future simulations to test is whether such MRi-like features can be created without causing such an unrealistically large distortion of the disk. This could be a matter of the particular accretion history of the simulated disk, and less massive satellites or particular infall trajectories could be more favorable. Including cold gas in simulated accretion events could affect the outcome, possibly absorbing energy of the infall or forming new stars within a distorted gas disk (as in, e.g., NGC 4565; Radburn-Smith et al. 2014). The behavior of the gas may also provide additional points of comparison between observations and simulations, as the warping of the H I disk is well-studied (Kalberla & Kerp 2009).

Additionally, a more comprehensive search of the available parameter space in the simulations could produce more realistic results. For example, the Kazantzidis et al. (2009) simulations were run until the disk had "settled," in that its bulk properties ceased to change significantly with time. While reasonable for understanding the properties of disks under bombardment in

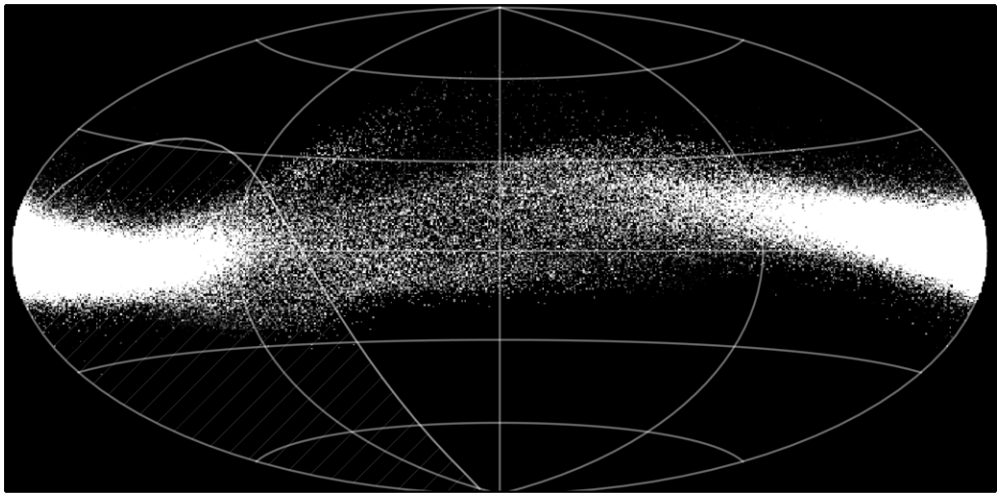

Figure 6. Visualization of the Kazantzidis et al. (2009) model, approximating the distance cut and uncertainties from the PS1 data in Figure 2. The feature annotations from Figure 3 have been included to give a sense of scale of the out of plane features. The hatched region indicates the area south of declination −30°, which is not observed by PS1. For clarity and as the model already includes a galactic disk, we have not overplotted it on the existing data. While the simulation is not designed to replicate individual features, there is a striking similarity between the model and the observed MRi in the presence of thin wisp-like features, but also a clearly excessive level of warping of the disk midplane beyond that seen in the Milky Way.

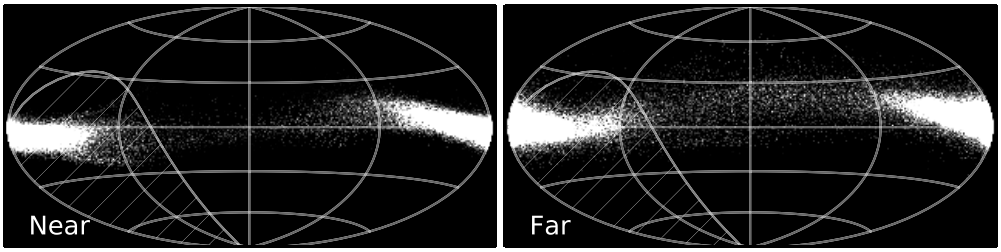

Figure 7. Visualization of Kazantzidis et al. (2009), showing a closer and a further distance cut (same as in Figure 4).

general, it is possible that we see the MRi today at a unique time in its dynamical evolution, and a search of multiple timesteps in a simulation may show transient effects (or possibly more evolved and settled states) that more closely resemble the MRi.

5. DISCUSSION AND CONCLUSIONS

Exploiting the photometric accuracy and 3π sky coverage of the PS1 photometry, we have presented the first distance-sensitive MSTO map of the Milky Way's stellar distribution at low ($|b| < 30^\circ$) Galactic latitudes. This map shows rich substructure, much of which has been referred to as the MRi structure in the past. This map (Figure 2) presents the most complete and only contiguous map of the MRi structure to date, showing its extent on both sides of the Galactic plane and covering over 130° in longitude. The characteristic sharp edge in density at large heights above the disk is readily distinguished on the northern and southern sides of the disk. The other arc-like features in the north have positions and morphologies that are suggestive of a connection to the MRi. The PS1 maps also suggest that the MRi is relatively confined in radius, and we find no evidence of new structures related to the MRi either closer to or further from the Sun.

It is not obvious how to decompose the structure we see in the MRi into a set of distinct components. If the structure is the remnant of a tidal disruption, its position along the Galactic disk certainly makes it challenging to recognize it as such. As we have discussed, the superposition of a stream atop the exponential density distribution of the disk could mask the signature of a stream. However, it is difficult to see how an orbit (or orbits) could yield a distribution of material over a narrow range in distance, since an accreted satellite must have fallen in from large distances. This observed behavior in distance is a strong constraint that future attempts to model an accretion event must agree with.

Likewise, it is difficult to intuitively understand what features are generated when a stellar disk is disrupted by satellites. It is likely that the state of the disk after such events is highly dependent on the mass and orbital parameters of the satellite (or satellites), and additionally is likely to be highly time-dependent. These difficulties in visualizing and modeling such events should not cause us to exclude them.

The challenges of understanding and recreating either formation scenario necessitate the use of models to both guide our understanding of the features we see and to provide predictions that can be used for differentiating between theories of the formation of such substructure. In both our comparisons to the accretion model of Peñarrubia et al. (2005) and perturbed disk model of Kazantzidis et al. (2009) we find qualitative agreement in reproducing some of the features of the MRi, but both also show areas of conflict with the observations. Our objective with the PS1 maps is to show where these models need improvement, and to show how even qualitative morphological constraints can be used to further refine the models of different formation scenarios.

Though we have explored two models that are particularly well-suited for comparison to the PS1 maps this is certainly not an exhaustive list of possible models for the MRi. There are also analytical models for the MRi that we have not considered in depth, such models that parameterize the structure as part of

a Galactic flare (Momany et al. 2006; Hammersley & López-Corredoira 2011). Proper consideration of these models requires a comprehensive fitting of the spatial and distance dependence of the observed distribution of disk stars as a whole, which is beyond the scope of this work. However, there are general morphological features of the flare models that we can compare to the observations. The sharp edge in latitude that has been characteristic of the MRi since its initial discovery, and which we have shown also exists prominently in the southern hemisphere, is a particularly strong constraint on Galactic flare models. Such a feature strongly suggests the existence of some dynamically cold component with a low velocity dispersion, which is at odds with flare models that require large vertical velocity dispersions to raise stars to greater heights above the disk.

Our presentation of these models is designed to link physical processes with the morphological features they create on the sky, demonstrating where these simulations perform best and drawing attention to where they most need refinement in order to plausibly explain the observed substructure. In the case of a tidal stream, we have shown that the challenge for future models is to limit the debris to a compact range of Galactocentric radii while still filling that range with a substantial amount of substructure. For perturbed disk models the goal must be to create substantial structures out of the plane without causing the disk to warp to such an unsupportable degree. The ability or inability of future models to accommodate these conditions as dictated by the data should help to narrow in on the origin of the MRi. This map provides an obvious starting point for follow-up observations, as three-dimensional velocities and metallicities of the stars in the various "features" should help to untangle their nature. Most of the stars should be bright enough to get good proper motion estimates from *Gaia*, but radial velocities and metallicities may require spectroscopy beyond the current set of spectroscopic surveys (RAVE, SEGUE, APOGEE, LAMOST, or *Gaia*). Nonetheless, it is clear that the Galactic disk offers a rich example of how galaxy disks are being disturbed, and how they respond to such disturbances.

We thank S. Kazantzidis for generously providing his simulation outputs. C.T.S. and E.F.B. were supported during this work by NSF grant AST 1008342. E.F.S., E.M., and N.F.M. acknowledge support from the DFG's SFB 881 grant "The Milky Way System" (sub-project A3). N.F.M. gratefully acknowledges the CNRS for support through PICS project PICS06183. H.W.R. acknowledges support from the European Research Council under the European Union's Seventh Framework Programme (FP 7) ERC grant Agreement no. [321035].

The PS1 Survey has been made possible through contributions of the Institute for Astronomy, the University of Hawaii, the Pan-STARRS Project Office, the Max-Planck Society and its participating institutes, the Max Planck Institute for Astronomy, Heidelberg and the Max Planck Institute for Extraterrestrial Physics, Garching, The Johns Hopkins University, Durham University, the University of Edinburgh, Queens University Belfast, the Harvard-Smithsonian Center for Astrophysics, and the Las Cumbres Observatory Global Telescope Network, Incorporated, the National Central University of Taiwan, and the National Aeronautics and Space Administration under grant No. NNX08AR22G issued through the Planetary Science Division of the NASA Science Mission Directorate.

Facility: PS1

REFERENCES

Belokurov, V., Zucker, D. B., Evans, N. W., et al. 2006, ApJL, 642, L137
Conn, B. C., Lane, R. R., Lewis, G. F., et al. 2007, MNRAS, 376, 939
Conn, B. C., Lane, R. R., Lewis, G. F., et al. 2008, MNRAS, 390, 1388
Conn, B. C., Lewis, G. F., Irwin, M. J., et al. 2005a, MNRAS, 362, 475
Conn, B. C., Martin, N. F., Lewis, G. F., et al. 2005b, MNRAS, 364, L13
Conn, B. C., Noël, N. E. D., Rix, H.-W., et al. 2012, ApJ, 754, 101
Crane, J. D., Majewski, S. R., Rocha-Pinto, H. J., et al. 2003, ApJL, 594, L119
de Jong, J. T. A., Yanny, B., Rix, H.-W., et al. 2010, ApJ, 714, 663
Frinchaboy, P. M., Majewski, S. R., Crane, J. D., et al. 2004, ApJL, 602, L21
García-Ruiz, I., Sancisi, R., & Kuijken, K. 2002, A&A, 394, 769
Gómez, F. A., Minchev, I., O'Shea, B. W., et al. 2013, MNRAS, 429, 159
Grillmair, C. J. 2006, ApJL, 651, L29
Grillmair, C. J. 2011, ApJ, 738, 98
Grillmair, C. J., Carlin, J. L., & Majewski, S. R. 2008, ApJL, 689, L117
Hammersley, P. L., & López-Corredoira, M. 2011, A&A, 527, A6
Ibata, R., Chapman, S., Ferguson, A. M. N., et al. 2005, ApJ, 634, 287
Ibata, R. A., Irwin, M. J., Lewis, G. F., Ferguson, A. M. N., & Tanvir, N. 2003, MNRAS, 340, L21
Kaiser, N., Burgett, W., Chambers, K., et al. 2010, Proc. SPIE, 7733, 77330E
Kalberla, P. M. W., & Kerp, J. 2009, ARA&A, 47, 27
Kazantzidis, S., Bullock, J. S., Zentner, A. R., Kravtsov, A. V., & Moustakas, L. A. 2008, ApJ, 688, 254
Kazantzidis, S., Zentner, A. R., Kravtsov, A. V., Bullock, J. S., & Debattista, V. P. 2009, ApJ, 700, 1896
Kroupa, P. 2001, MNRAS, 322, 231
Li, J., Newberg, H. J., Carlin, J. L., et al. 2012, ApJ, 757, 151
Magnier, E. 2006, The Advanced Maui Optical and Space Surveillance Technologies Conference, ed. S. Ryan (Maui, HI: Economic Development Board), E50
Martin, N. F., Ibata, R. A., Bellazzini, M., et al. 2004, MNRAS, 348, 12
Martin, N. F., Ibata, R. A., Rich, R. M., et al. 2014, ApJ, 787, 19
Martin, N. F., Irwin, M. J., Ibata, R. A., et al. 2006, MNRAS, 367, L69
Mateu, C., Vivas, A. K., Zinn, R., Miller, L. R., & Abad, C. 2009, AJ, 137, 4412
Meisner, A. M., Frebel, A., Jurić, M., & Finkbeiner, D. P. 2012, ApJ, 753, 116
Metcalfe, N., Farrow, D. J., Cole, S., et al. 2013, MNRAS, 435, 1825
Momany, Y., Zaggia, S., Gilmore, G., et al. 2006, A&A, 451, 515
Newberg, H. J., Yanny, B., Rockosi, C., et al. 2002, ApJ, 569, 245
Newby, M., Newberg, H. J., Simones, J., Cole, N., & Monaco, M. 2011, ApJ, 743, 187
Peñarrubia, J., Martínez-Delgado, D., Rix, H. W., et al. 2005, ApJ, 626, 128
Pietrinferni, A., Cassisi, S., Salaris, M., & Castelli, F. 2004, ApJ, 612, 168
Purcell, C. W., Bullock, J. S., Tollerud, E. J., Rocha, M., & Chakrabarti, S. 2011, Natur, 477, 301
Radburn-Smith, D. J., de Jong, R. S., Streich, D., et al. 2014, ApJ, 780, 105
Richardson, J. C., Ferguson, A. M. N., Johnson, R. A., et al. 2008, AJ, 135, 1998
Rocha-Pinto, H. J., Majewski, S. R., Skrutskie, M. F., Crane, J. D., & Patterson, R. J. 2004, ApJ, 615, 732
Sanchez-Saavedra, M. L., Battaner, E., & Florido, E. 1990, MNRAS, 246, 458
Schlafly, E. F., & Finkbeiner, D. P. 2011, ApJ, 737, 103
Schlafly, E. F., Finkbeiner, D. P., Jurić, M., et al. 2012, ApJ, 756, 158
Schlegel, D. J., Finkbeiner, D. P., & Davis, M. 1998, ApJ, 500, 525
Slater, C. T., Bell, E. F., Schlafly, E. F., et al. 2013, ApJ, 762, 6
Sollima, A., Valls-Gabaud, D., Martinez-Delgado, D., et al. 2011, ApJL, 730, L6
Vivas, A. K., & Zinn, R. 2006, AJ, 132, 714
Widrow, L. M., Gardner, S., Yanny, B., Dodelson, S., & Chen, H.-Y. 2012, ApJL, 750, L41
Yanny, B., Newberg, H. J., Grebel, E. K., et al. 2003, ApJ, 588, 824
Younger, J. D., Besla, G., Cox, T. J., et al. 2008, ApJL, 676, L21